Available online at www.sciencedirect.com

SciVerse ScienceDirect

Scripta Materialia 65 (2011) 1085–1088

Scripta MATERIALIA

www.elsevier.com/locate/scriptamat

Three-dimensional visualization of material flow during friction stir welding by two pairs of X-ray transmission systems

Y. Morisada,* H. Fujii, Y. Kawahito, K. Nakata and M. Tanaka

Joining and Welding Research Institute, Osaka University, Ibaraki, Osaka 567-0047, Japan

Received 29 July 2011; revised 14 September 2011; accepted 15 September 2011
Available online 20 September 2011

Material flow during friction stir welding is crucial to obtaining sound joints. However, this phenomenon is still not fully understood despite many investigations and numerous models. In this study, the material flow is three-dimensionally visualized by X-ray radiography using a tiny spherical tungsten tracer. The movement of the tracer during the friction stir welding is observed by two pairs of X-ray transmission real-time imaging systems. The three-dimensional material flow is obtained by following the locus of the tracer.

Keywords: Friction stir welding; Radiography; Material flow; Visualization

Recently, much attention has been paid to friction stir welding (FSW). FSW is a solid-state joining technique in which a rotating tool is inserted into the interface at the butt line of metal plates and produces a highly plastically deformed zone. The metal plates are joined as the rotating tool travels along the interface. It is well known that FSW joints show excellent mechanical properties because of the recrystallized fine and equiaxed grains in the stir zone. Therefore, FSW has been widely developed as a spot joining and surface modification technique. Various surface composites have also been also fabricated by friction stir processing (FSP).

The material flow around the rotating tool during FSW/FSP is the key to obtaining a sound joint and modified region. The material flow has been studied using various approaches because an accurate understanding of this phenomenon can lead to optimization of the process conditions. In the first study of this type, Colligan used small steel shots set at different positions in aluminum sheet to estimate the material flow [1]. The material flow was subsequently investigated by the tracking of a tracer [2–5], observation of the flow pattern in a weld of dissimilar materials [6–9], analysis of the crystallographic texture in a weld [10], and by measuring the eutectic Si distribution [11]. X-ray computer tomography has been used to try to observe the dispersion of various tracers after FSW [2,12]. However, the material flow during FSW is still unclear. It is difficult to gain an accurate picture of the material flow using these approaches because the experimental results obtained show only one part of the process. In situ observation by an X-ray radiography technique seems to be a very effective with which to study the material flow [13]. In this paper, the material flow is three-dimensionally visualized using a 300 μm spherical tungsten tracer. The three-dimensional material flow is obtained using the locus of the tungsten tracer observed by two pairs of X-ray transmission real-time imaging systems.

A schematic drawing of the experimental set-up for the X-ray radiography during FSW is shown in Figure 1. A pure aluminum (A1050) plate was used as the workpiece. The workpiece and the backplate were both 5 mm thick. The unthreaded tool, which has a columnar shape (15.0 mm diameter) with a probe (6.0 mm diameter, 1.9 mm long), was used for the FSW. A2017 and Si_3N_4 were chosen as materials for the backplate and the tool for FSW, respectively. X-rays can transmit through the workpiece, the backplate and the tool due to their low relative densities (Al: 2.7 g cm^{-3}, Si_3N_4: 3.4 g cm^{-3}). The two pairs of X-ray transmission real-time imaging systems were set to fix the perspective center in the middle of the stir zone. Both lines of the X-ray passed through the horizontal A1050 plate at an angle of 30° each. The X-ray transmission images were recorded by two high-speed video cameras at the frame rate of 500 fps. These video cameras were synchronized to obtain a three-dimensional graph using the locus of the tracer observed

* Corresponding author. E-mail: morisada@jwri.osaka-u.ac.jp

1359-6462/$ - see front matter © 2011 Acta Materialia Inc. Published by Elsevier Ltd. All rights reserved.
doi:10.1016/j.scriptamat.2011.09.021

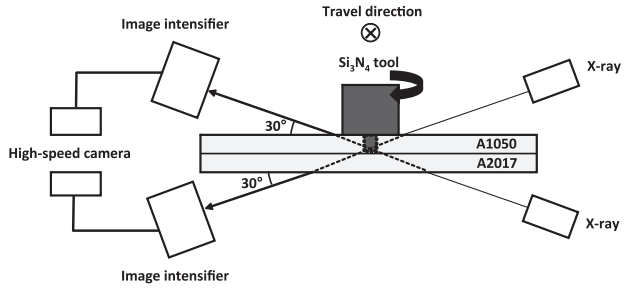

Figure 1. A schematic drawing of the experimental set-up for the X-ray radiography during FSW.

by the two imaging intensifiers. Figure 2 shows the two X-ray transmission images. The tungsten tracer, which was under the tool shoulder, can be clearly observed in both images. It was set at 1 mm from the top surface of the A1050 plate before the FSW. The 0.8 mm diameter hole was formed by drilling for the tracer arrangement. The diameter of the tungsten tracer was about 300 μm. Figure 2a was taken from the upper side of the plate with an X-ray tube voltage of 100 kV and a tube current of 8 mA. Figure 2b was taken from the lower side of the plate with an X-ray tube voltage of 180 kV and a tube current of 1 mA. Although image (a) was brighter than image (b), the resolution of image (b) was higher than that of image (a).

FSW was carried out in positional control mode. The rotation rate and the travel rate of the tool were 400 mm min^{-1} and 1000 rpm, respectively. A tool tilt angle of 3° was used. Figure 3 shows the three-dimensional graph and various two-dimensional graphs obtained using the coordinates of the tungsten tracer. WD, TD and ND show the welding direction of the FSW, the transverse direction of the A1050 plate, and the normal direction of the A1050 plate, respectively. The material flow around the probe was essentially similar to that reported in previous studies [14]. However, surprisingly the tungsten tracer rotated around the probe seven times. This result implied that the assumption that the material flow was based on the final position of the tracer was not entirely accurate. The velocity of the tungsten tracer and the peripheral velocity of the tool were not same, as will be shown later. The flow zone of almost the same 2 mm width around the probe, regardless of the rotating and travel directions of the tool, could be confirmed on the WD–TD graph. There was no difference between the advancing side (AS) and retreating side (RS). On the other hand, the downward movement of the tungsten tracer was confirmed on the other graphs. A 300 μm spherical molybdenum tracer was used to investigate the effect of the tracer density on the material flow. The downward movement was hardly observed for the molybdenum tracer because of its lower relative density of 10.3 g cm^{-3}. Therefore, it is considered that the high relative density of the tungsten tracer (19.3 g cm^{-3}) led to the downward movement, which was not affected by the original material flow. The horizontal material flow around the probe was tilted against the travel direction as shown in the ND–WD graph. The tilt of the horizontal flow can be explained by the combination of the horizontal flow and the convectional flow generated at the rear of the probe by the shoulder [3].

The velocity of the tungsten tracer at RS, AS, the backward side (BS) and the forward side (FS) is shown in Figure 4. The three-dimensional coordinates of the tungsten tracer can be obtained from the two pairs of X-ray transmission real-time imaging systems. The velocity of the tungsten tracer was directly calculated by the change in the coordinate over 0.002 s on the WD–TD plane. The tungsten tracer gradually moved to the outer side of the stir zone due to centrifugal force. There was no significant difference in the velocity on all sides, and it increased with the distance from the center of the probe. The velocities near the probe were lower than the peripheral velocity of the probe, which was 314.0 mm s^{-1}. These values expressed as a ratio of the tool peripheral velocity showed good agreement with the tracer velocities reported by Schmidt et al. [2]. However, the velocity at RS reached 339.0 mm s^{-1} which was higher than the peripheral velocity of the probe. It is considered that the velocity of the horizontal material flow was affected by both the probe and the shoulder. Therefore, the velocity on the outer side was higher than that of the inner side in the stir zone. The peripheral velocity at the periphery of the shoulder was 785.0 mm s^{-1}. Indeed, all the calculated velocities were lower than the peripheral velocity at the periphery of the shoulder.

The velocity at RS was slightly higher than that at AS at the same distance from the center of the probe. The difference of 6.7 mm s^{-1} (400 mm min^{-1}) can be easily explained by the relative velocity between the travel direction and the rotation of the tool. However, the difference between the velocity at RS and AS seems to be

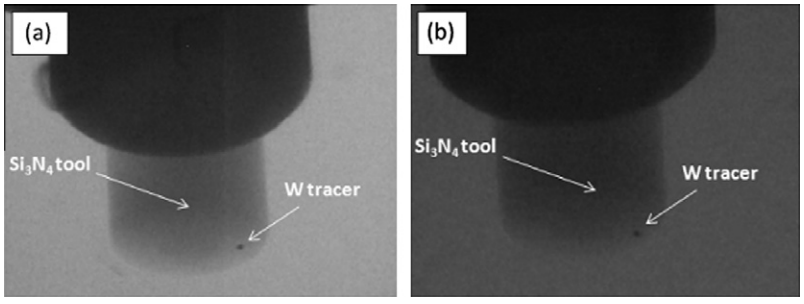

Figure 2. X-ray transmission images obtained by the X-ray transmission real-time imaging systems: (a) image from the upper side of the plate; (b) image from the lower side of the plate.

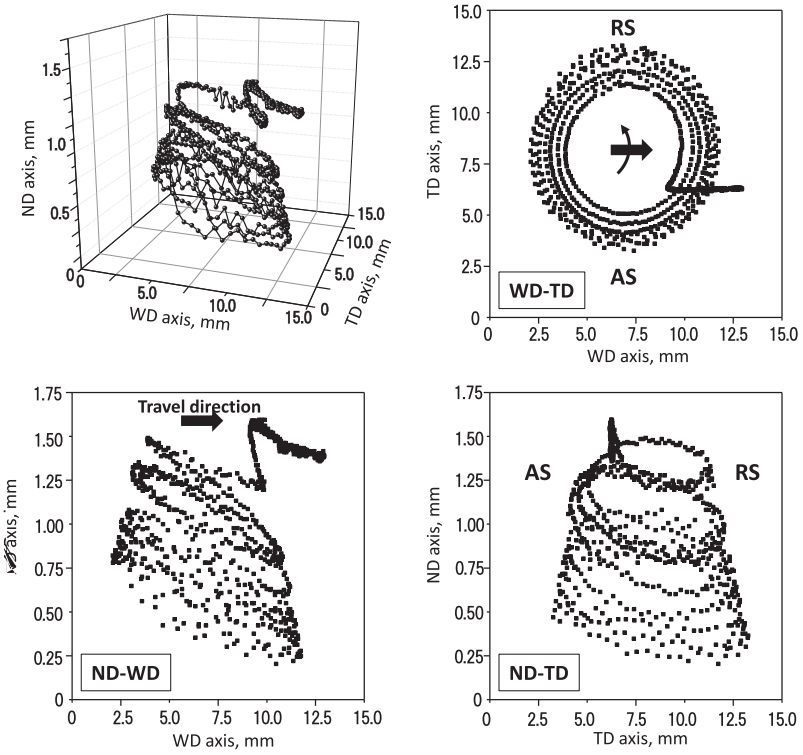

Figure 3. A three-dimensional graph and various two-dimensional graphs obtained using the coordinates of the tungsten tracer.

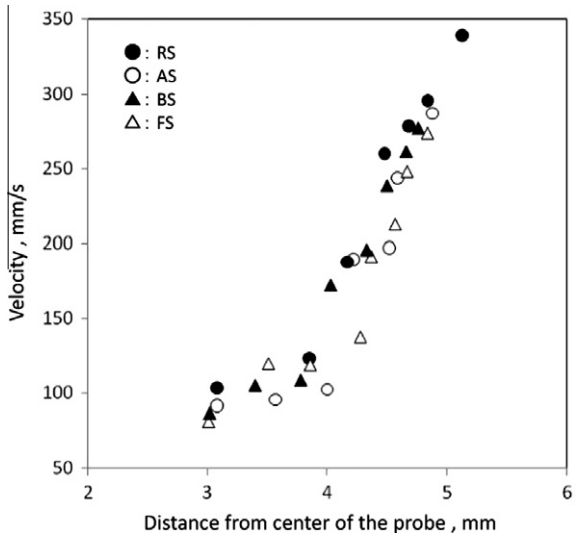

Figure 4. The velocity of the tungsten tracer.

$\sim$20 mm s^{-1}, which is larger than 6.7 mm s^{-1}. The relatively high pressure created by the tool traveling at the front of the probe is likely to be one of the reasons for the lower velocity at AS.

In summary, the material flow during FSW was successfully visualized by X-ray radiography. A three-dimensional graph was obtained using the locus of the tungsten tracer observed by two pairs of X-ray transmission real-time imaging systems. Although a high density of the tungsten tracer led to a slight downward movement which was not attributed to the material flow, the profile of the material flow around the tool was clearly observed. The results can be summarized as follows:

(1) There was a flow zone with a uniform width around the probe.
(2) The horizontal round flow around the probe was tilted by the convectional flow.
(3) The velocity of the material flow on the outer side was higher than that on the inner side in the stir zone.
(4) The velocity at RS was slightly higher than that at AS at the same distance from the center of the probe.

This study was supported by Priority Assistance for the Formation of Worldwide Renowned Centers of Research—The Global COE Program (Project: Center of Excellence for Advanced Structural and Functional Materials Design), and by a Grant-in-Aid from the Ministry of Education, Culture, Sports, Science and Technology (MEXT), Japan. Additionally, this study was supported by the Japan Science and Technology Agency (JST) under Collaborative Research Based on Industrial Demand "Heterogeneous Structure Control: Towards Innovative Development of Metallic Structural Materials".

[1] K. Colligan, Welding J. 78 (1999) 229.
[2] H.N.B. Schmidt, T.L. Dickerson, J.H. Hattel, Acta Mater. 54 (2006) 1199.
[3] Y. Morisada, H. Fujii, T. Nagaoka, K. Nogi, M. Fukusumi, Composites A 38 (2007) 2097.
[4] A.P. Reynolds, Scripta Mater. 58 (2008) 338.
[5] O. Lorrain, V. Favier, H. Zahrouni, D. Lawrjaniec, J. Mater. Process. Technol. 210 (2010) 603.

[6] Y. Li, L.E. Murr, J.C. McClure, Mater. Sci. Eng., A 271 (1999) 213.
[7] M. Guerra, C. Schmidt, J.C. McClure, L.E. Murr, A.C. Nunes, Mater Character 49 (2003) 95.
[8] P. Su, A. Gerlich, T.H. North, G.J. Bendzsak, Metall. Mater. Trans. A 38A (2007) 584.
[9] B.C. Liechty, B.W. Webb, J. Mater. Process. Technol. 184 (2007) 240.
[10] K. Kumar, S.V. Kailas, Mater. Sci. Eng., A 485 (2008) 367.
[11] H. Fujii, Y.G. Kim, T. Tsumura, T. Komazaki, K. Nakata, Mater. Trans. 47 (2006) 224.
[12] R. Zettler, T. Donath, J.F. dos Santos, F. Beckman, D. Lohwasser, Adv. Eng. Mater. 8 (2006) 487.
[13] Y. Kawahito, M. Mizutani, S. Katayama, J. Phys. D Appl. Phys. 40 (2007) 5854.
[14] R. Nandan, T. DebRoy, H.K.D.H. Bhadeshia, Prog. Mater. Sci. 53 (2008) 980.